Waveguide-hologram-based wavelength-multiplexed pseudoanalog true-time-delay module for wideband phased-array antennas

Zhenhai Fu, Charles Zhou, and Ray T. Chen

A pseudoanalog true-time-delay (TTD) module based on substrate-guided waves and wavelength-division multiplexing is presented. A 1-to-32 (5-bit) even fan-out is demonstrated by use of a two-dimensional waveguide hologram array. This module has a packing density of 2.5 lines/cm^2 and very compact packaging (8 cm $\times$ 4 cm $\times$ 8 mm). It also reduces TTD system complexity by providing continuously tuned delay signals to parallel-control the whole phased-array antenna system. The device has a measured bandwidth of as high as 2.4 THz. The delay signal can range from tens of picoseconds to several nanoseconds. © 1999 Optical Society of America

OCIS codes: 050.7330, 060.4230, 200.4650.

1. Introduction

Phased-array antennas (PAA's), which combine the signals from up to thousands of stationary antenna elements with the same frequency, can be scanned electronically by means of reprogramming the signals fed to the individual elements. PAA's have the potential for a wide variety of applications from surveillance, tracking, astronomy, and geodesy to wireless and satellite communications. The use of phased arrays has been severely limited because phase-shifting electronics are intrinsically narrow band. Replacing phase shifts with true time delays (TTD's) allows the microwave phase shift at each antenna element, which is proportional to the microwave frequency, to follow the frequency change without creating drift in the beam-steering angle.[1–3] Therefore signals from different antenna elements can be correlated without frequency dependence.

For real system implementations of TTD beam steering a specific beam-forming direction is achieved by selection of a TTD setting. To scan the beam into another angle, it is necessary to establish a completely different configuration of the delays. Most existing TTD beam-steering systems adopt two approaches.[2–4] First, the array elements are grouped into subarrays; each subarray shares a common time delay. Second, each time-delay unit is built to provide a discrete set of delay lines. The set of discrete time-delay increments selected for each steering angle represents a quantized approximation to a linear phase taper. Photonic systems promise a means of obtaining the beam agility of array systems combined with a wide bandwidth, a compact size, reduced weight, a low high-frequency rf loss, and lower electromagnetic interference.[3]

Various types of photonic TTD delay units, such as fiber delay lines,[4–7] fiber optical Bragg grating TTD elements,[8,9] waveguide optical time-shift networks,[10–12] acousto-optic TTD elements,[13] wavelength-multiplexed TTD lines,[14–17] and free-space TTD lines,[18–20] have been demonstrated by a few research groups. These TTD lines do have some advantages such as accurate time delays and monolithic integration with detectors, but they suffer from some disadvantages such as a need for many light sources, switches, and modulators, a low packing density, complexity in fabrication and control, and high loss.

2. Structure of Substrate-Guided-Wave True-Time-Delay Lines

Our previous papers[21–23] reported two-dimensional substrate-guided-wave TTD modules operating at 850 nm that were designed and fabricated to provide successive optical delays of as long as $32\Delta\tau$. Figure

The authors are with the Microelectronics Research Center, The University of Texas at Austin, Austin, Texas 78758. R. T. Chen's e-mail address is raychen@uts.cc.utexas.edu.

Received 31 July 1998; revised manuscript received 27 October 1998.

0003-6935/99/143053-07$15.00/0

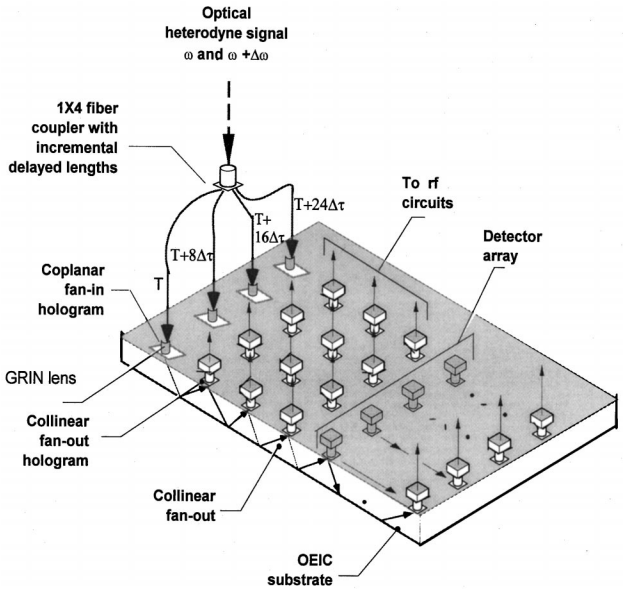

Fig. 1. Diagram of the structure of 5-bit TTD lines based on a substrate-guided mode with holographic-grating couplers. OEIC, optoelectronic integrated circuit; GRIN, graded index.

1 illustrates the basic system architecture of our 5-bit device. A 1-to-4 fiber beam splitter with predetermined output fiber lengths is used to provide four delay signals, each with an $8\Delta\tau$-delay increment. Each delay signal from the 1-to-4 beam splitter is coupled into the substrate surface normally with a specific substrate bounce angle through a holographic coupler and then zigzags within the substrate through total internal reflection. Portions of the substrate-guided waves are extracted sequentially and surface normally through holographic output-coupler arrays.

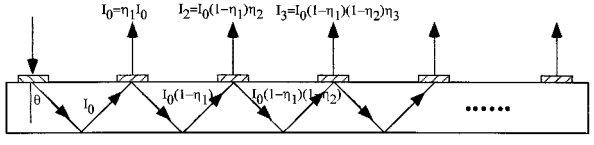

Fig. 2. Substrate-guided-wave optical TTD line with a surface-normal configuration.

Figure 2 illustrates the structure of one of the four TTD subunits with delay paths provided by cascaded substrate-guided optical fan-outs. The input holographic-grating coupler is designed to couple the surface-normal incoming TEM_{00} heterodyned optical signal into a substrate-guided mode. The output holographic-grating couplers extract an array of substrate-guided beams into a free-space one-dimensional array that has eight surface-normal fan-out beams. Different optical delays are obtained at subsequent fan-outs within the substrate. Equivalent delay intervals are obtained at subsequent fan-outs as a result of equivalent propagation-distance differences. The time delay between two successive collinear fanouts is $\Delta\tau$. Thus $32(2^5)$ delay lines are achieved. The fan-out optical signals are detected by a high-speed photodetector array and then sent to antenna transmitters by means of programmed switching.

To illustrate the implementation of the device shown in Fig. 2, we used a 5-bit module as four 3-bit units to control a PAA with five antenna subarrays (one of the five subarrays is provided with a zero-delay signal), as shown in Fig. 3. Each subarray has four antenna elements that share the same delay signals. A phase shifter is placed behind each antenna element to fine-tune the phase delays and therefore to scan with a small angular increment. Similarly, suppose the PAA is programmed to steer in an angular range from $+45°$ to $-45°$. The possible scanning angles and the corresponding delay signals needed by each subarray are listed in Table 1 with $\Delta\tau$ set at 50 ps. As shown in Fig. 3 and Table 1, to look in one direction, say $-45°$, we see that the microwave switches behind the subarrays connect the desired delay signals of 0, $8\Delta\tau$, $16\Delta\tau$, $24\Delta\tau$, and $32\Delta\tau$ to subarrays 1, 2, 3, 4, and 5, respectively. To look in

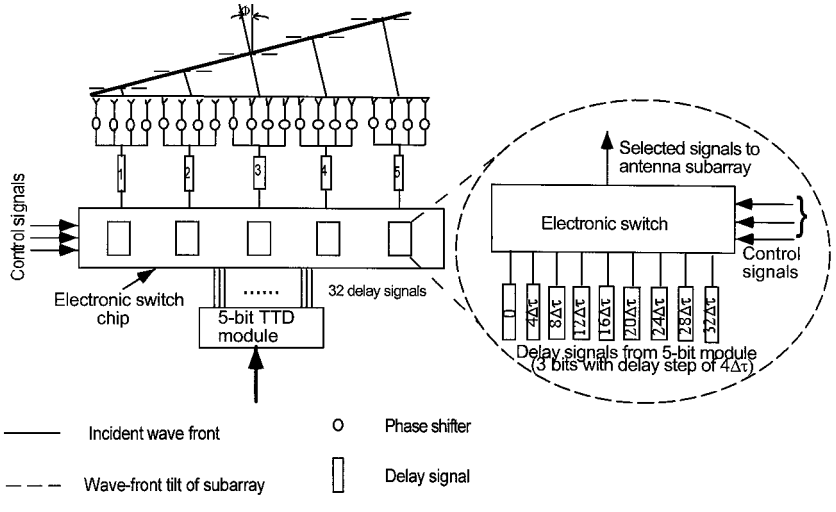

Fig. 3. One 5-bit TTD module that controls one PAA with five subarrays.

Table 1. Scanning Angles and the Corresponding Delays of Each Subarray

	Subarray						Subarray				
Scanning Angle	1	2	3	4	5	Scanning Angle	1	2	3	4	5
−45°	0	8Δτ	16Δτ	24Δτ	32Δτ	45°	32Δτ	24Δτ	16Δτ	8Δτ	0
−38.2°	0	7Δτ	14Δτ	21Δτ	28Δτ	38.2°	28Δτ	21Δτ8	14Δτ	7Δτ	0
−32°	0	6Δτ	12Δτ	18Δτ	24Δτ	32°	24Δτ	18Δτ	12Δτ	6Δτ	0
−26.2°	0	5Δτ	10Δτ	15Δτ	20Δτ	26.2°	20Δτ	15Δτ	10Δτ	5Δτ	0
−20.7°	0	4Δτ	8Δτ	12Δτ	16Δτ	20.7°	16Δτ	12Δτ	8Δτ	4Δτ	0
−15.4°	0	3Δτ	6Δτ	9Δτ	12Δτ	15.4°	12Δτ	9Δτ	6Δτ	3Δτ	0
−10.2°	0	2Δτ	4Δτ	6Δτ	8Δτ	10.2°	8Δτ	6Δτ	4Δτ	2Δτ	0
−5.1°	0	1Δτ	2Δτ	3Δτ	4Δτ	5.1°	4Δτ	3Δτ	2Δτ	1Δτ	0
0	0	0	0	0	0	0	0	0	0	0	0
Delay step	0	Δτ	2Δτ	3Δτ	4Δτ	Delay step	4Δτ	3Δτ	2Δτ	Δτ	0

another direction, say +32°, we find that the switches controlled by the control signals send delay signals of 24Δτ, 18Δτ, 12Δτ, 6Δτ, and 0 to the corresponding subarrays. For scanning into angles not listed in Table 1, the delay signal that is closest to the desired delay signal can be used instead. For example, if 2.8Δτ is needed, 3Δτ will be used instead. In such an arrangement the antenna array can be controlled easily by one 5-bit TTD module and an electronic switch chip instead of five different 3-bit TTD modules with different delay steps. Similarly, a 6-bit TTD module based on the structure described above can serve as eight 3-bit units or four 4-bit units. And one 7-bit module can serve as sixteen 3-bit units, eight 4-bit units, or four 5-bit units, and so on. Therefore the signal loss is much lower and the weight and the cost of the system are reduced dramatically.

3. Characteristics of Holographic-Grating Couplers

The structure of a volume holographic Bragg grating[24] for surface-normal coupling is shown in Fig. 4. The grating induced by the refractive-index modulation is slanted with a tilt angle of ϕ. The grating spacing is Λ. The incident angle and the diffraction angle to the surface-normal direction are α and θ, respectively. The grating designed by use of the phase-matching condition satisfies the following:

$$2k \sin\left(\frac{\alpha + \theta}{2}\right) = K, \tag{1}$$

where $k = 2\pi n/\lambda$ is the wave vector and $K = 2\pi/\Lambda$ is the grating vector.

For any designed thick grating the phase-matching condition is strictly true for only one wavelength. Because the input angle and the grating vector are fixed, the phase-matching condition will deviate from the perfect phase-matching condition for wavelengths that differ from the designed center wavelength. By taking a derivative of the diffraction angle with respect to the wavelength with the input angle fixed, we can write the angular deviation $\Delta\theta$ of the diffraction angle with respect to the perfect phase-matching diffraction angle as

$$\Delta\theta = \frac{\Delta\lambda}{\lambda} \tan\theta. \tag{2}$$

The dispersion relation derived in Eq. (2) can also be derived from constructive interference of the surface gratings, as defined by

$$\frac{\Lambda}{\sin\phi}(\sin\alpha + \sin\theta) = \frac{\lambda}{n}. \tag{3}$$

To evaluate the accuracy of Eq. (2), we used a Clark Model MXR NTA-5 femtosecond mode-locked laser composed of a wide spectrum (an approximately 50-nm, 3-dB bandwidth). The laser pulse is surface-normally coupled into the Bragg grating coupler fabricated on a DuPont Series HRF-600×20 photopolymer with a peak diffraction efficiency of as much as 99%. The grating is slanted and is designed for surface-normal input at the center wavelength of 833 nm. The diffraction angle is 45° in a BK-7 waveguiding plate ($n = 1.509$). The cw composition of the laser pulse is coupled out dispersively by a fused-silica prism ($n = 1.453$) that has a negligible dispersion effect compared with the polymer grating. The diffraction pattern of a mode-locked

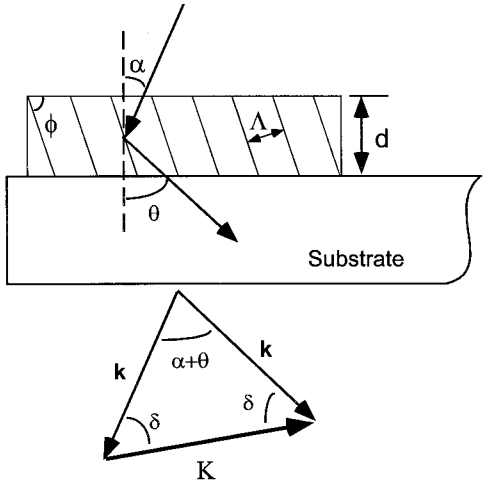

Fig. 4. Structure of a surface-normal holographic-grating coupler.

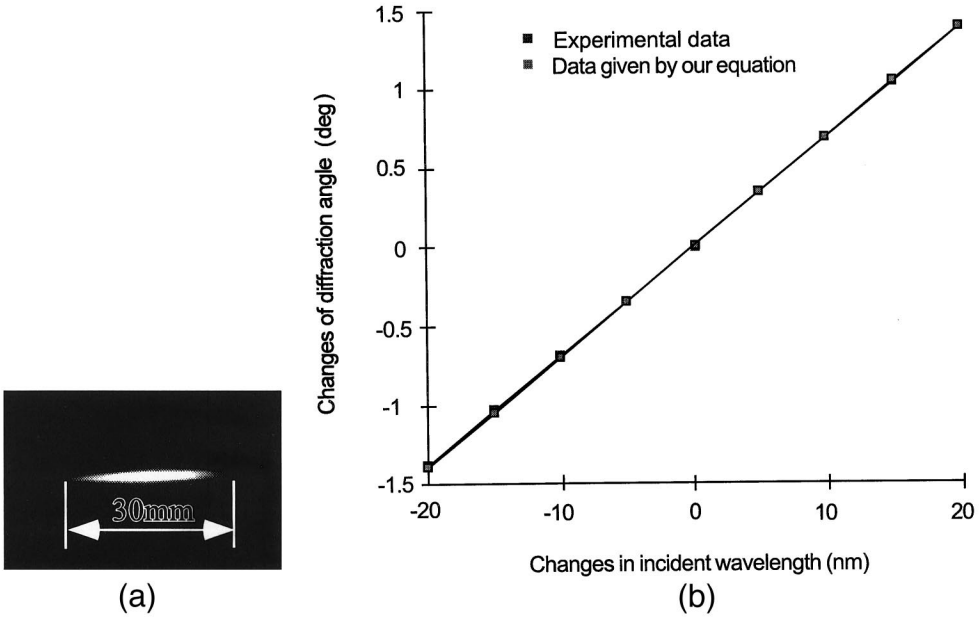

Fig. 5. (a) Dispersion spot of a mode-locked femtosecond laser. (b) Experimental dispersion data for a thick holographic grating.

laser pulse with a pulse width of 300 fs and a detectable bandwidth of $\delta\lambda \approx 40$ nm is shown in Fig. 5(a). Experimental data of the light dispersion are obtained by measurement of the wavelengths versus the corresponding diffracted dot positions. With the known refractive indices of the materials the diffraction angles of the TM wave versus the corresponding wavelengths are calculated and plotted in Fig. 5(b) together with the dispersion angle predicted with Eq. (2). The theoretical and the experimental angular-dispersion data are found to be matched perfectly within $\pm 1\%$ for both TE and TM waves.[25]

4. Wavelength-Multiplexed Pseudoanalog True-Time-Delay Lines

From verified Eq. (2), we note that, if the wavelength of the beam incident upon the structure shown in Fig. 2 changes slightly, the corresponding diffraction angle within the substrate will follow this change, as shown in Fig. 6. As a result the length of the optical delay path after n bounces will change slightly, which causes the signal delay to change in a small range. For the central wavelength the delay between two successive bounces is given by

$$\Delta\tau = \frac{2hn}{(\cos\theta)C}, \tag{4}$$

where h is the height of the substrate, n is the refractive index of the substrate (1.528 at 1550 nm), C is the velocity of light in free space, and θ is the bounce angle in the substrate. For a value of θ of approximately 45° the delay between two successive bounces will change with the operating wavelength by an amount given by

$$\Delta'\tau = \frac{2hn\sin\theta}{(\cos^2\theta)C}\Delta\theta = \frac{2hn\sin\theta}{(\cos^2\theta)C}\frac{\Delta\lambda}{\lambda}\tan\theta$$

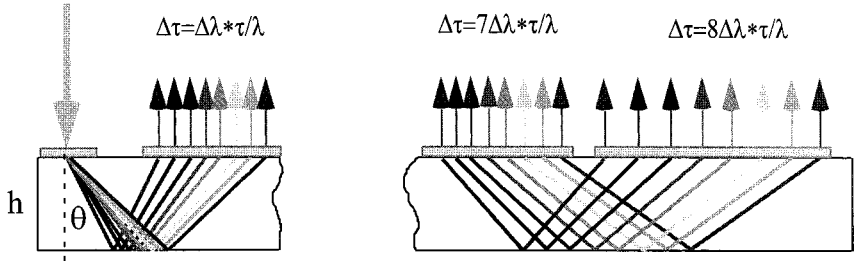

Fig. 6. Structure of wavelength-multiplexed TTD lines.

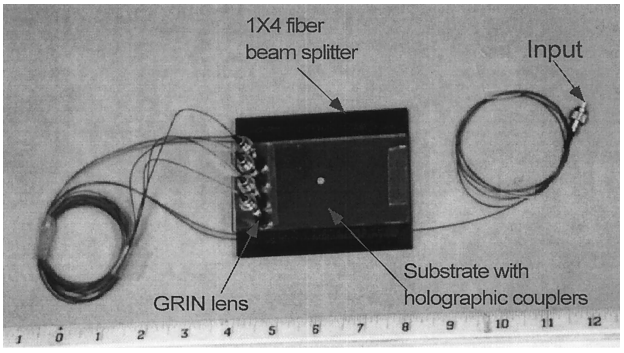

(a)

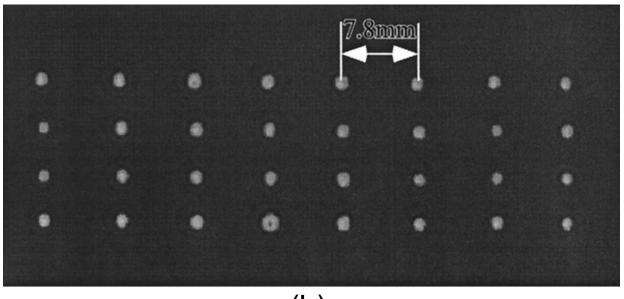

(b)

Fig. 7. (a) Photograph of the packaged 5-bit TTD module. Scale in inches. (b) Thirty-two fan-outs from the TTD modules.

$$\approx \frac{2hn}{(\cos\theta)C}\frac{\Delta\lambda}{\lambda} = \Delta\tau\frac{\Delta\lambda}{\lambda}. \tag{5}$$

Therefore we can continuously tune the delay step by tuning the operating wavelength instead of the quantized value.

By replacing the four output fibers from the 1×4 fiber beam splitter of Fig. 1 with a highly dispersive fiber that has the same dispersion characteristics as that of the substrate-guided-wave devices that employ a tunable laser source, we can achieve continuous delay tuning around 32 discrete signal delays, and only 32 detectors are needed to detect all the delay signals from the TTD module. The fan-outs under different operating wavelengths need to be grouped and focused onto the small sensitive areas of the high-speed photodetectors.

As described in Section 2, one 5-bit module can be used as four 3-bit units to steer the beam of a PAA with five antenna subarrays into 17 discrete directions within the $\pm 45°$ range under one wavelength. After the configuration of the delay signals is set to steer the radiated beam to one discrete direction, continuous scanning in a small range around this discrete direction can be achieved by means of continuous tuning of the operating wavelength around the central wavelength.

From Table 1 let us suppose that the delay step between two antenna elements for the mth scanning

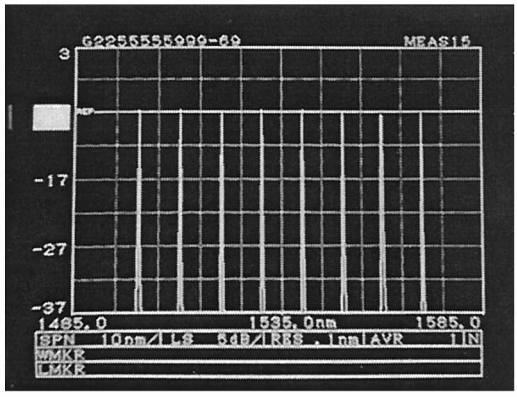

(a)

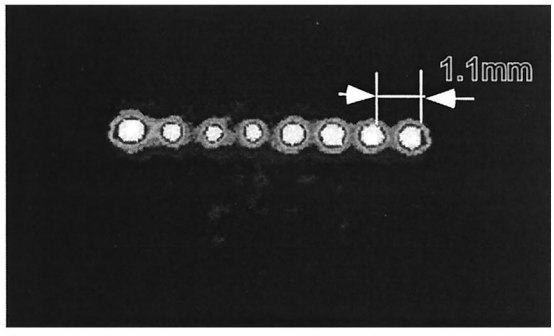

(b)

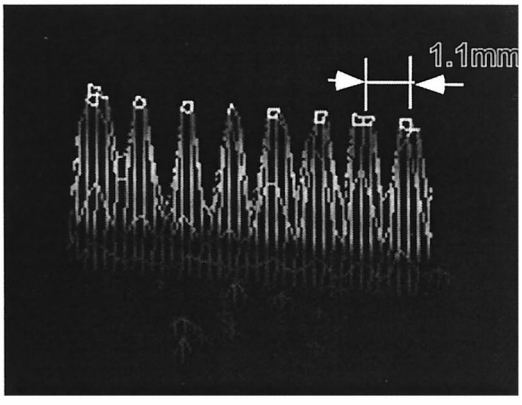

(c)

Fig. 8. (a) Spectrum diagram of the sampled wavelengths. (b) Two-dimensional plot of the fan-out spots after eight bounces under different wavelengths. (c) Three-dimensional plot of the fan-out spots after eight bounces under different wavelengths.

angle is τ_m and the smallest delay step under the center wavelength is $\Delta\tau$. We then have

$$\tau_m = m\Delta\tau, \tag{6}$$

$$\Delta\tau_m = m\Delta\tau\frac{\Delta\lambda}{\lambda} = m\Delta'\tau. \tag{7}$$

Therefore

$$\tau_m' = m\Delta\tau\left(\frac{\Delta\lambda}{\lambda} + 1\right). \tag{8}$$

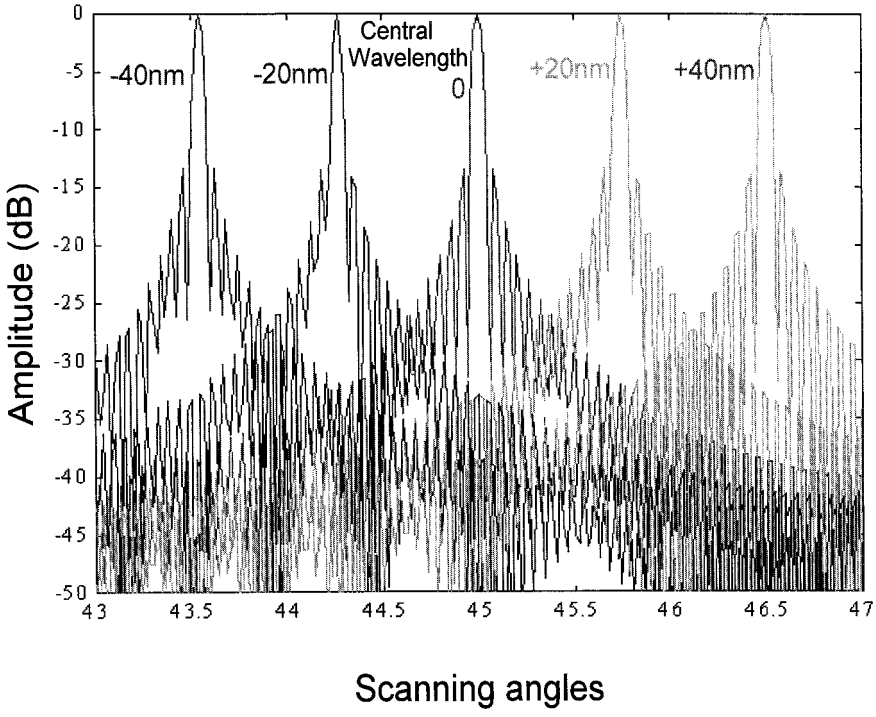

Fig. 9. Far-field patterns of a PAA with 128 elements under different operating wavelengths.

To achieve continuous scanning, i.e., a continuous delay step, it is necessary to satisfy the following:

$$\tau_m - \Delta\tau_m = \tau_{m-1} + \Delta\tau_{m-1}, \tag{9}$$

i.e.,

$$m\Delta\tau - m\Delta\tau\frac{\Delta\lambda}{\lambda} = (m-1)\Delta\tau + (m-1)\Delta\tau\frac{\Delta\lambda}{\lambda}. \tag{10}$$

Therefore the required minimum wavelength change is given by

$$\frac{\Delta\lambda}{\lambda} = \frac{1}{2m-1}. \tag{11}$$

5. Experimental Results

A packaged 5-bit TTD module composed of a 1×4 fiber beam splitter and a quartz substrate with a holographic-grating coupler is shown in Fig. 7(a). The substrate thickness of the waveguiding plate is 3 mm, and the substrate bounce angle is 52.3°, which yields a distance between two successive fan-outs of 7.8 mm and a delay step of 50 ps. The operating wavelength is approximately 1550 nm, which makes it easy to amplify the optical signals by use of commercially available erbium-doped fiber amplifiers. The 32 resultant fan-out spots are shown in Fig. 7(b). The device has a measured bandwidth of as high as 2.5 THz[23] and a packing density of 2.5 lines/cm^2. The total insertion loss, including the 1-to-32 fan-out loss, is less than 20 dB.

Tuning the incident wavelength around 1550 nm will move the positions of the fan-out spots along the propagation direction. Figure 8(a) shows a spectrum diagram of the sampled wavelength, and the corresponding fan-out spots after eight bounces are shown in Figs. 8(b) and 8(c) in two-dimensional and three-dimensional formats, respectively.

With one input wavelength the distance between two successive fan-outs is given by

$$L = 2h\tan\theta. \tag{12}$$

The position change with wavelength is

$$\Delta L = \frac{d(2\tan\theta)}{d\lambda}\Delta\lambda = \frac{2h\sin\theta}{\cos^3\theta} * \frac{\Delta\lambda}{\lambda}. \tag{13}$$

In our case $\theta = 52.3°$, $\lambda = 1550$ nm, $h = 3$ mm, and the number of bounces is 8; therefore

$$\frac{\Delta L}{\Delta\lambda} = 0.107 \text{ mm/nm}, \tag{14}$$

which is very close to the experimental result shown in Fig. 8. The simulated far-field patterns of a PAA with 128 elements, which can be realized fully on the basis of the reported data under different operating wavelengths, are shown in Fig. 9. It is obvious that the scanning direction changes continuously with the operating wavelength.

6. Conclusion

In summary a wavelength-multiplexed 5-bit substrate-guided-wave TTD module that can provide continuously tuned delay signals for continuous steering of the beam radiated from PAA's has been proposed, fabricated, and experimentally confirmed.

This module has a packing density of 2.5 lines/cm^2, a bandwidth of 2.4 THz, and very compact packaging (8 cm $\times$ 4 cm $\times$ 8 mm).

This research is currently supported by the Office of Naval Research, the U.S. Air Force Research Laboratory, the Advanced Research Projects Agency, 3M Foundation, and the Advanced Technology Program of the State of Texas.

References

1. A. A. Oliner and G. H. Knittel, *Phased Array Antennas* (Artech House, Norwood, Mass., 1972).
2. R. J. Mailloux, *Phased Array Antenna Handbook* (Artech House, Norwood, Mass., 1993).
3. H. Zmuda and E. N. Toughlian, *Photonic Aspect of Modern Radar* (Artech House, Norwood, Mass., 1994).
4. W. Ng, A. A. Walston, G. L. Tangonan, J. J. Lee, I. L. Newberg, and N. Bernstein, "The first demonstration of an optically steered microwave phased array antenna using true-time-delay," J. Lightwave Technol. **9,** 1124–1131 (1991).
5. E. Ackerman, S. Wanuga, D. Kasemset, W. Minford, N. Thorsten, and J. Watson, "Integrated 6-bit photonic true-time-delay unit for lightweight 3–6 GHz radar beamformer," IEEE Trans. Microwave Theory Tech. **6,** 681–684 (1992).
6. K. Kang, K. Deng, S. Koehler, I. Glesk, and P. Prucnal, "Fabrication of precision fiber-optic time delays with *in situ* monitoring for subpicosecond accuracy," Appl. Opt. **36,** 2533–2536 (1997).
7. R. Y. Loo, G. L. Tangonan, H. W. Yen, J. J. Lee, V. L. Jones, and J. Lewis, "5 bit photonic time shifter for wideband arrays," Electron. Lett. **31,** 1521–1522 (1996).
8. G. A. Ball, W. H. Glenn, and W. W. Morey, "Programmable fiber optic delay line," IEEE Photonics Technol. Lett. **6,** 741–743 (1994).
9. J. L. Cruz, B. Ortega, M. V. Andres, B. Gimeno, D. Paster, J. Capmany, and L. Dong, "Chirped fiber Bragg gratings for phased-array antennas," Electron. Lett. **33,** 545–546 (1997).
10. S. Yegnanarayanan, P. D. Trink, and B. Jalali, "Recirculating photonic filter: a wavelength-selective time delay for phased-array antennas and wavelength code-division multiple access," Opt. Lett. **21,** 740–742 (1996).
11. W. Ng, R. Loo, V. Jones, and J. Lewis, "Silica-waveguide optical time-shift network for steering a 96-element *L*-band conformal array," in *Optical Technology for Microwave Applications III*, A. P. Goutzoulis, ed., Proc. SPIE **2560,** 140–147 (1995).
12. W. Ng, D. Yap, A. Narayanan, A. Walston, and R. Hayes, "Detector-switched GaAs monolithic time-delay network for the optical control of phased arrays," in *Proceedings of the IEEE Lasers and Electro-Optics Society Annual Meeting* (Institute of Electrical and Electronics Engineers, New York, 1993), pp. 211–212.
13. L. H. Gesell, R. E. Feinleib, J. L. Lafuse, and T. M. Turpin, "Acousto-optic control of time delays for array beam steering," in *Optoelectronic Signal Processing for Phased-Array Antennas IV*, B. M. Hendrickson, ed., Proc. SPIE **2155,** 194–204 (1994).
14. D. T. K. Tong and M. C. Wu, "A novel multiwavelength optically controlled phased array antenna with a programmable dispersion matrix," IEEE Photonics Technol. Lett. **8,** 812–814 (1996).
15. R. Esman, M. Frankel, J. Dexter, L. Goldberg, M. Parent, D. Stilwell, and D. Cooper, "Fiber-optic prism true time-delay antenna feed," IEEE Photonics Technol. Lett. **5,** 1347–1349 (1993).
16. A. Goutzoulis, D. Davies, and J. Zomp, "Hybrid electronic fiber optic wavelength-multiplexed system for true time-delay steering of phased array antennas," Opt. Eng. **31,** 2312–2322 (1992).
17. R. Soref, "Optical dispersion technique for time-delay beam steering," Appl. Opt. **31,** 7395–7397 (1992).
18. H. R. Fetterman, Y. Chang, D. C. Scott, S. R. Forrest, F. M. Espiau, M. Wu, D. V. Plant, J. R. Kelly, A. Mather, and W. H. Steier, "Optically controlled phased array radar receiver using SLM switched real time delays," IEEE Microwave Guid. Wave Lett. **5,** 414–416 (1995).
19. D. Dolfi, P. Joffre, J. Antoine, J. Huignard, D. Philippet, and P. Granger, "Experimental demonstration of a phased-array antenna optically controlled with phase and time delays," Appl. Opt. **35,** 5293–5300 (1996).
20. I. Frigyes and A. Seeds, "Optically generated true-time delay in phased-array antennas," IEEE Trans. Microwave Theory Tech. **43,** 2378–2386 (1995).
21. R. Li, Z. Fu, and R. Chen, "High packing density 2.5 THz true-time-delay lines using spatially multiplexed substrate guided waves in conjunction with volume holograms on a single substrate," J. Lightwave Technol. **15,** 2253–2258 (1997).
22. Z. Fu, R. Li, and R. Chen, "Compact broadband 5-bit photonic true-time-delay module for phased array antennas," Opt. Lett. **23,** 522–524 (1998).
23. Z. Fu and R. Chen, "Five-bit substrate guided wave true-time delay module working at up to 2.4 THz with a packing density of 2.5 lines/cm^2 for phased array antenna applications," Opt. Eng. **37,** 1838–1844 (1998).
24. C. Zhou, Z. Fu, M. Dubinovsky, J. I. R. Chen, and P. Dempewolf, "Dispersion enhanced wavelength division multiplexing," in *Optoelectronic Interconnects and Packaging IV*, R. T. Chen and S. Guilfoyle, eds., Proc. SPIE **3005,** 144–154 (1997).
25. C. Zhou, Z. Fu, R. T. Chen, and B. Davies, "Dispersion correction of surface-normal optical interconnection using two compensated holograms," Appl. Phys. Lett. **72,** 3249–3251 (1998).